AGU PUBLICATIONS

Geophysical Research Letters

RESEARCH LETTER
10.1002/2017GL073656

Key Points:
- During austral spring 2016 total Antarctic sea ice extent decreased at a record rate that was 18% faster than previously observed
- The most anomalous sea ice retreat took place during November and in the Weddell and Ross Sea sectors
- Record surface pressure anomalies occurred during spring, with the most negative November Southern Annular Mode index since 1968

Supporting Information:
- Supporting Information S1

Correspondence to:
J. Turner,
jtu@bas.ac.uk

Citation:
Turner, J., T. Phillips, G. J. Marshall, J. S. Hosking, J. O. Pope, T. J. Bracegirdle, and P. Deb (2017), Unprecedented springtime retreat of Antarctic sea ice in 2016, *Geophys. Res. Lett.*, *44*, 6868–6875, doi:10.1002/2017GL073656.

Received 31 MAR 2017
Accepted 31 MAY 2017
Accepted article online 20 JUN 2017
Published online 10 JUL 2017

Unprecedented springtime retreat of Antarctic sea ice in 2016

John Turner[1], Tony Phillips[1], Gareth J. Marshall[1], J. Scott Hosking[1], James O. Pope[1], Thomas J. Bracegirdle[1], and Pranab Deb[1]

[1]British Antarctic Survey, Natural Environment Research Council, Cambridge, UK

Abstract During austral spring 2016 Antarctic sea ice extent (SIE) decreased at a record rate of 75×10^3 km^2 d^{-1}, which was 46% faster than the mean rate and 18% faster than in any previous spring season during the satellite era. The decrease of sea ice area was also exceptional and 28% greater than the mean. Anomalous negative retreat occurred in all sectors of the Antarctic but was greatest in the Weddell and Ross Seas. Record negative SIE anomalies for the day of year were recorded from 3 November 2016 to 9 April 2017. Rapid ice retreat in the Weddell Sea took place in strong northerly flow after an early maximum ice extent in late August. Rapid ice retreat occurred in November in the Ross Sea when surface pressure was at a record high level, with the Southern Annular Mode at its most negative for that month since 1968.

1. Introduction

Since the late 1970s the Arctic sea ice extent (SIE) has decreased at a significant rate [*Serreze and Stroeve*, 2015], with a number of record low extents being observed in recent years [*Parkinson and Comiso*, 2013]. However, over the same period, the total Antarctic SIE increased at a small but significant rate [*Fetterer et al*., 2002; *Simmonds*, 2015; *Parkinson and DiGirolamo*, 2016], although this masked large regional variations. A number of mechanisms have been put forward to explain this increase in SIE [*Zhang*, 2007; *Turner et al*., 2009; *Bintanja et al*., 2013; *Ferreira et al*., 2015; *Holland et al*., 2017]; however, based on preindustrial control runs of coupled climate models, the trend does seem to be within the bounds of natural climate variability [*Turner et al*., 2013a]. In September 2012 Antarctic SIE reached a new maximum for the satellite era (beginning in 1979) [*Turner et al*., 2013b], with further records being observed in 2013 [*Reid et al*., 2015] and 2014. However, over austral spring (September–November) 2016 Antarctic SIE decreased at a record rate, resulting in a SIE anomaly of -2.25×10^6 km^2 by the end of November. Following the record spring SIE retreat, the extent of ice stayed at low levels and culminated on 1 March 2017 with the Antarctic total SIE dropping to 2.07×10^6 km^2—the lowest level in a record starting in 1979.

SIE is often held up as an important indicator of climate change, with models projecting that Arctic sea ice will decrease markedly over the 21st century if greenhouse gas concentrations continue to increase [*Zhang and Walsh*, 2006]. The positive trend of Antarctic SIE since the 1970s, when greenhouse gas concentrations have been increasing to levels not experienced in the last 20 Ma [*Zachos et al*., 2008], has therefore prompted a great deal of debate over the magnitude of the intrinsic variability of Antarctic SIE and the detection of anthropogenic signals at high southern latitudes [*Hawkins and Sutton*, 2009]. The fact that the Antarctic SIE is decreasing over 1979–2005 in the vast majority of Coupled Model Intercomparison Project Phase 5 model historical runs also makes the observed increase all the more surprising [*Turner et al*., 2013a]. The record rate of springtime SIE retreat in 2016 is a further challenge to our understanding of sea ice variability in the relatively short observational record of Antarctic SIE.

In this paper we investigate why the retreat of Antarctic sea ice was so rapid in spring 2016. We consider the role of atmospheric circulation anomalies in advecting relatively warm air masses into the sea ice zone and briefly discuss the possible role of the ocean.

2. Data

We examine the sea ice evolution using daily and monthly mean extent and area data from the U.S. National Snow and Ice Data Center (www.nsidc.org). Sea ice area is taken as the sum of the area of each satellite pixel multiplied by the sea ice concentration. Sea ice extent is the total area of all satellite pixels where the sea ice

concentration equals or exceeds 15%. We have used the sea ice data produced using the NASA Team algorithm 1.1 [*Cavalieri et al*., 1984] since these data are available from National Snow and Ice Data Center as a consistent time series covering 1979 to 2015. Prior to 1987 data are only available every other day, so data for missing days were produced by linear interpolation for each pixel between the fields for the previous and next days. For 2016 and 2017 we have used the NASA Team near-real-time (NRT) data. These data are affected by data quality issues including missing pixels over the ocean (both individual scattered pixels and missing swaths), small regions erroneously identified as sea ice and (in a single case) a broad region of sea ice clearly inconsistent with the data for the previous and next days. We minimized the impact of these issues using a two-stage process. First, we performed a manual inspection of each field, flagging regions that appeared erroneous as either 0% sea ice concentration or as missing pixels as appropriate. We then estimated values for the missing pixels. If a missing pixel had at least two nearest neighbors in the same field that were not missing, we estimated its value as the mean of the nearest neighbor values. Otherwise, if a missing pixel had data values in the fields for both the previous and the next day, we estimated its value as the mean of these values. If neither of these methods could be applied, the pixel was left as missing. A comparison between the final NASA sea ice data and the NRT data for 2014 and 2015 that had our corrections applied showed that the differences were small enough on the regional scale to give us confidence in their use here.

We examine SIE and sea ice area for the Southern Ocean as a whole and for five sectors that have been considered in a number of earlier studies [e.g., *Zwally et al*., 2002]. These are the Ross Sea (160°E–130°W), Amundsen-Bellingshausen Sea (ABS) (130°W–60°W), Weddell Sea (60°W–20°E), Indian Ocean (20°E–90°E), and western Pacific Ocean (90°E–160°E). Sea ice anomalies for 2016 were computed using climatological fields for 1979–2015. Note that no sea ice data are available for the period 3 December 1987 to 12 January 1988 so we have excluded data for the extended melt season of 1987/88 spanning August 1987 to March 1988 in the computation of the means. This ensured that the sample size of melt seasons is consistent over the 38 year record.

Atmospheric circulation was examined using the European Centre for Medium-range Weather Forecasts (ECMWF) Interim (ERA-Interim) reanalysis fields. These were produced with a consistent analysis scheme throughout the record [*Dee et al*., 2011] and were interpolated onto a 1.125° × 1.125° (~125 km) grid. The ERA-Interim fields are reliable across high southern latitudes from 1979 and are considered to be the best reanalysis data set for depicting recent Antarctic climate [*Bracegirdle and Marshall*, 2012].

The SAM index was taken from https://legacy.bas.ac.uk/met/gjma/sam.html, where the data are available from 1957. As described in *Marshall* [2003], the index was computed from surface meteorological observations from Antarctic coastal and Southern Ocean island stations.

3. Antarctic Sea Ice Retreat

Over 1979–2015 the total Antarctic SIE had a mean maximum extent of 18.67×10^6 km^2, with the mean day of maximum being 21 September (Figure 1a), with a standard deviation of 9 days. However, the day of maximum SIE has varied markedly, with the earliest and latest dates prior to 2016 being 31 August (1994) and 3 October (1988), respectively. September is usually a month of net SIE increase, with the mean advance being 0.26×10^6 km^2 (Table 1), although retreats have occurred during 32% of the years since 1979. In the following months there has always been retreat for the Antarctic as a whole, with the mean total SIE change being -1.19×10^6 km^2 (October), -3.73×10^6 km^2 (November), and -6.62×10^6 km^2 (December) (Table 1). While the largest mean monthly SIE decrease is in December, this is also the month of greatest variability of decrease, with a standard deviation (SD) of 0.70×10^6 km^2 and a range of SIE change from -4.92×10^6 km^2 (2007) to -8.04×10^6 km^2 (2010).

Sea ice retreat does not take place at the same rate and time in all sectors of the Antarctic (Figure S1a in the supporting information). On average, SIE in the Indian Ocean sector increases more than any other region in September but experiences by far the greatest absolute retreat in November, with the retreat being more than twice the magnitude of any other sector. In contrast, the Weddell Sea dominates the retreat in October but has only half the ice loss of the Indian Ocean sector by November. By the end of the melt season almost all sea ice in the Indian Ocean and Pacific sectors has melted, while ice usually persists in the ABS and Ross Sea, and especially the Weddell Sea, which has the greatest amount of multiyear sea ice.

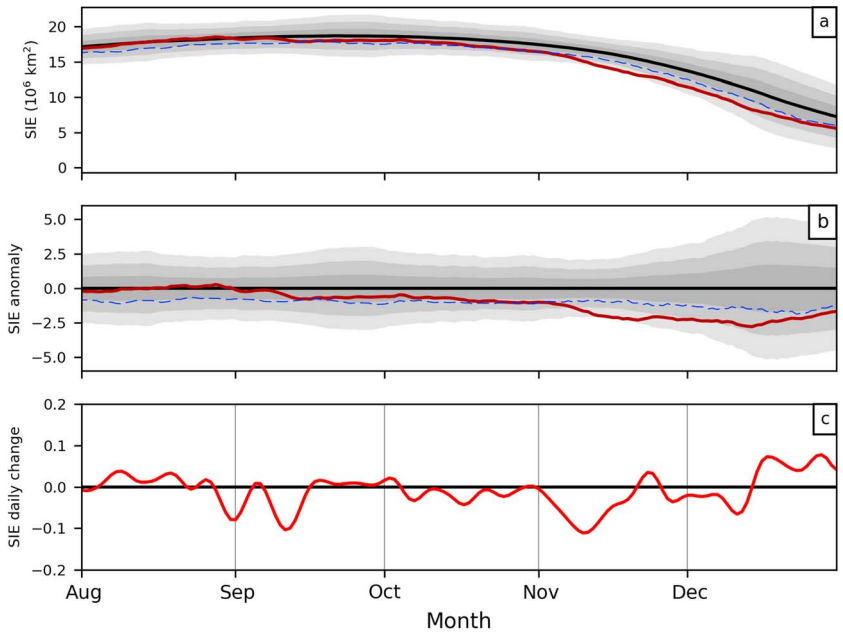

Figure 1. (a) The daily total Antarctic SIE for August–December showing the 2016 data (red) and the 1979–2015 mean (black). (b) The 2016 daily SIE anomaly and (c) the daily change of the 10 day smoothed 2016 SIE. The ±2, 4, and 6 standard deviations are indicated in Figures 1a and 1b. The broken blue lines in Figures 1a and 1b indicate the lowest daily SIE and SIE anomaly values over 1979–2015.

The annual mean extent of the sea ice in the five sectors is influenced by different aspects of the atmospheric circulation [*Turner et al.*, 2015]. The variability in the Ross Sea, Weddell Sea, and ABS is strongly modulated by changes in the depth and location of the Amundsen Sea Low (ASL) [*Hosking et al.*, 2013], while SIE in the West Pacific Ocean sector is more influenced by atmospheric circulation anomalies immediately to the north of this region. SIE variability in the Indian Ocean sector is strongly related to a SAM-like pattern of mean sea level pressure (MSLP) anomalies, with greater SIE associated with the positive phase of the SAM [see *Turner et al.*, 2015, Figure 3].

Greater total Antarctic SIE decrease in September/October is associated with a more positive SAM-like pattern of lower MSLP over Antarctica and higher MSLP over midlatitudes, which is associated with stronger westerly winds over the Southern Ocean (Figure S2). It is also associated with a wave number 3 pattern of anomalies, which leads to marked meridional flow in certain sectors [*Turner et al.*, 2016]. In September the greatest ice decrease takes place in the ABS (Figure S1a), and a deeper ASL (the mean location in September is centered near 135°W, 72°S) gives enhanced northerly flow and greater warm air advection to the west of the Antarctic Peninsula, so promoting early ice decrease in this region. In October, when ice loss is dominated by change in the Weddell Sea, low MSLP over this region promotes ice transport around the Weddell Sea gyre and into more northerly latitudes just to the east of the Antarctic Peninsula, where the warmer ocean temperatures lead to greater sea ice melt. The circulation pattern promoting greater sea ice

Table 1. The Change (Difference in Extent Between the First Day of the Month/Season and the First Day of the Next Month/Season) (10^6 km^2) in SIE During August–December and Spring (September–November) 2016 for the Whole Southern Ocean and the Five Sectors, Along With the Mean Change Over 1979–2015 in Parentheses

	August	September	October	November	December	Spring
Weddell Sea	0.63 (0.36)	−0.31 (0.04)	−0.53 (−0.52)	−1.54 (−0.76)	−3.01 (−2.57)	−2.38 (−1.24)
Indian Ocean	0.22 (0.49)	0.36 (0.27)	−0.32 (−0.17)	−1.42 (−1.29)	−1.16 (−1.65)	−1.38 (−1.20)
West Pacific Ocean	0.02 (0.10)	−0.15 (0.07)	−0.18 (−0.17)	−0.68 (−0.67)	−0.16 (−0.45)	−1.01 (−0.78)
Ross Sea	0.27 (0.15)	0.13 (0.02)	−0.46 (−0.19)	−0.94 (−0.64)	−1.20 (−1.34)	−1.27 (−0.80)
ABS	0.21 (0.13)	−0.26 (−0.14)	−0.12 (−0.14)	−0.40 (−0.36)	−0.47 (−0.61)	−0.78 (−0.64)
Total Southern Ocean	1.34 (1.24)	−0.23 (0.26)	−1.61 (−1.19)	−4.99 (−3.73)	−5.99 (−6.62)	−6.82 (−4.66)

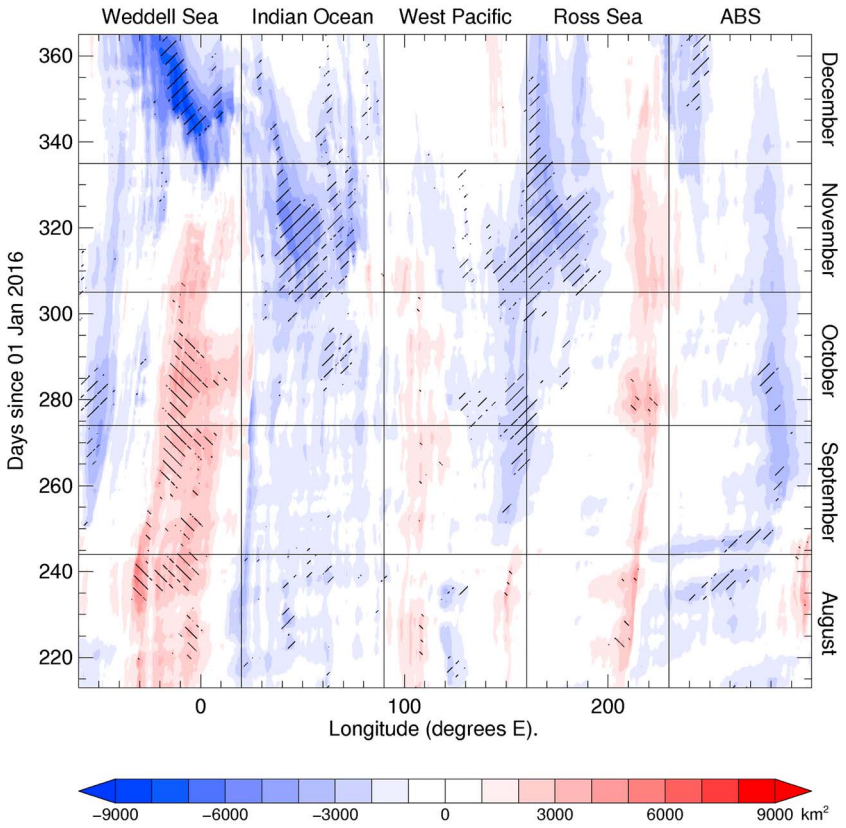

Figure 2. A time-longitude plot of sea ice extent anomaly for August–December 2016. The color scale refers to anomalies in 0.2° longitude sectors. The hashed areas indicate where the anomalies relative to the years 1979–2015 (excluding 1987) were at a record level.

loss in November (Figure S2c) is quite different from the previous 2 months and consists of negative SAM-like MSLP anomalies of high MSLP over the Antarctic and low pressure over midlatitudes. This pattern reflects the dominance of the Indian Ocean sector in controlling the total Antarctic SIE during November and the dependence of SIE in this sector on the phase of the SAM. The greater decrease of SIE when the SAM is negative is consistent with larger poleward heat flux when the SAM is in this phase, as noted by *Marshall and Thompson* [2016], and reduced Ekman flow [*Hall and Visbeck*, 2002].

4. The Anomalous Sea Ice Retreat in 2016

Over the spring months of September to November 2016 the Antarctic SIE decreased by 6.82×10^6 km^2, which was 46% greater than the mean loss and 18% more than in any previous spring season during the satellite era (Table 1). The decrease in sea ice *area* over this period was also exceptional at 6.44×10^6 km^2, which was 28% more than the mean and 4% larger than in any previous spring. The SIE anomaly was consistently negative after 1 September and at least 2 SD below the mean from 17 October to the end of the year, with record low daily extents every day from 3 November (Figure 1b).

The evolution of the SIE anomalies from August 2016 to the end of the year is illustrated via the time/longitude plot in Figure 2. Overall, there was a high persistence of anomalies throughout the period, with little zonal translation of the anomalies, although the faint patterns progressing eastward at approximately 10° per day reflect the influences of mobile weather systems. One of the most long-lived anomalies occurred in the Weddell Sea sector, where there was a large positive slowly eastward moving anomaly from August to November, which then rapidly switched to a large negative westward moving anomaly in December. These changes are consistent with positive sea ice anomalies in the north of the Weddell Sea and negative anomalies in the south advected around the Weddell gyre. Long-lived negative anomalies were also found in the Indian Ocean and ABS sectors, while the West Pacific and Ross Sea sectors had more transient anomalies.

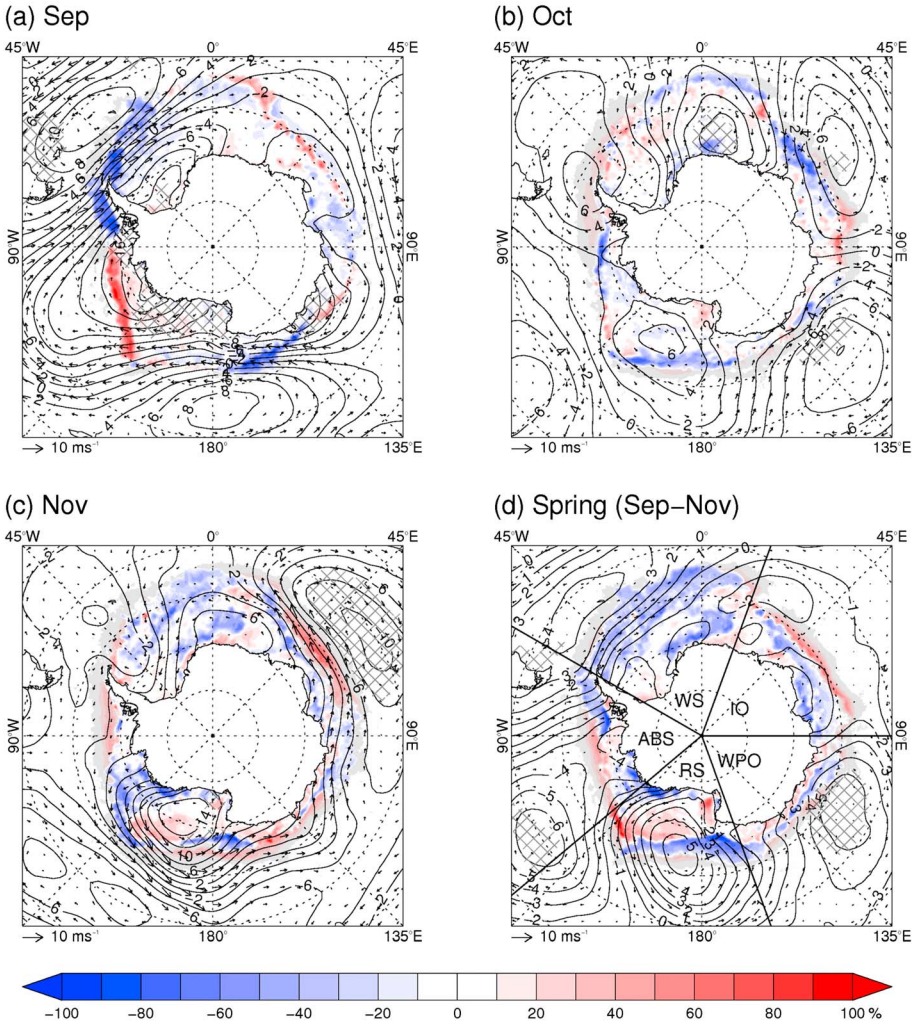

Figure 3. Anomalous sea ice concentration change, MSLP and 10 m winds for (a) September, (b) October,(c) November, and (d) spring. Gray cross hatching indicates where the mean MSLP over the period shown in 2016 falls outside the range of equivalent MSLP values in any of years 1979–2015. Gray partially transparent masking shows where the reduction in sea ice concentration in 2016 was less than the mean loss for the equivalent period over 1979–2015 but where the sea ice concentration at the end of the period in 2016 was 0%. Figure 3d also shows the five sectors discussed in the text. IO = Indian Ocean, WPO = West Pacific Ocean, RS = Ross Sea, ABS = Amundsen-Bellingshausen Sea, and WS = Weddell Sea.

During 2016 the Antarctic SIE maximum was on 28 August, which was the earliest day of maximum in the record, and there was an overall SIE change during September of -0.23×10^6 km^2 (the mean change is an increase of 0.27×10^6 km^2) (Table 1). During September the SAM was positive and MSLP in the area of the ASL was deeper than in any September in the ERA Interim data starting in 1979 (960 hPa compared to a mean of 976 hPa) (Figure 3a). The deep ASL gave strong northwesterly flow across the ABS and northwestern Weddell Sea and contributed to the marked retreat of sea ice west of the Antarctic Peninsula and across the northern Weddell Sea (Table 1). The SIE in the ABS sector experienced almost double its usual September retreat (Table 1), while the SIE in the Weddell Sea decreased more than in any other sector. However, the mean monthly SIE for the Weddell Sea was slightly more than the climatological mean (Table S1) because of the positive anomaly at the start of the month (Figure 2).

The decrease in total Antarctic SIE during September was dominated by a drop in extent of 0.54×10^6 km^2 between 7 and 14 September (Figures 1b and 1c), with the greatest retreat taking place over this period in the Weddell Sea and West Pacific sectors. A mobile depression that tracked eastward from the ABS into the southern Weddell Sea was responsible for the change in the Weddell Sea sector. In the West Pacific sector the greatest ice retreat was associated with a very deep depression (<932 hPa) that gave strong

northerly flow across the area over 11–13 September. The SIE decrease over 7–14 September was large, but not the largest 7 day SIE decrease ever observed in September. Following this period of rapid SIE decrease, the magnitude of the negative anomaly reduced, so that by the end of the month the total Antarctic SIE was low, but only the sixth smallest extent in the record.

During October 2016 Antarctic SIE decreased by 35% more than the mean rate. At this time there was strong meridional flow in a number of sectors (Figure 3b), with greater onshore flow and sea ice retreat, in the Ross Sea, Indian Ocean and ABS. By the end of the month the SIE was 16.47×10^6 km^2, which was the second lowest extent for October after 1986.

While the decrease of sea ice during September and October was more rapid than normal, the most anomalous retreat took place in November. During this month SIE decreased by 4.99×10^6 km^2, which was the largest November retreat in the satellite era, and 34% larger than the mean. The most rapid retreat took place during the first 3 weeks, with the SIE on 18 November being 5.82 SD below the multiannual mean for that day.

The greatest contribution to the overall November SIE retreat came from the Weddell Sea sector, which accounted for over 62% of the -1.26×10^6 km^2 total anomaly. At the start of the month there was a positive SIE anomaly of 0.18×10^6 km^2, which was a legacy of the positive SIE anomalies in the region that had been present throughout the winter, reaching a peak on 28 August. On 1 November most of the ice extent anomaly was eastward of 40°W, and this gradually declined during the month as negative anomalies increased over the western Weddell Sea. These changes in SIE anomaly were a result of a couplet of low and high MSLP anomalies that were present centered respectively on 45°W and 0° (Figure 3c), which gave anomalous northeasterly flow and marked poleward heat flux (not shown) over the eastern Weddell Sea. Climatologically, sea ice concentration in this sector starts to decrease close to the Greenwich Meridian in the vicinity of the Maud Rise (the Maud Rise polynya), with the negative anomalies spreading into the eastern Weddell Sea and down the coast of Dronning Maud Land. During November 2016 the ice concentrations in the vicinity of the Maud Rise and off the coast of Dronning Maud Land were lower than normal (Figure S3), although the lower ice extent in this area only contributed about 7% to the total anomaly of the sector. There were also anomalously low ice concentrations during this month across the northern part of the Weddell Sea (Figure S3), which will have aided the rapid retreat of ice.

The other sector that contributed significantly (~24%) to the ice retreat anomaly in November was the Ross Sea. Here the monthly mean MSLP just north of the Ross Ice Shelf was at a record level of $>$14 hPa above the mean, giving onshore flow close to 170°E and offshore flow near 130°W (Figure 3c). Warm air advection on the western side of the positive MSLP anomaly decreased the ice extent over the month through a combination of ice compaction and melt. The strong offshore flow from West Antarctica advected ice away from the coast creating a coastal polynya, which also contributed to the decrease of SIE in this sector over the course of the month.

The November SAM index of -3.12, as derived from observational data [*Marshall*, 2003], was the most negative November value since 1968 in a record starting in 1957, with positive MSLP anomalies over the Antarctic and negative anomalies in midlatitudes (Figure 3c). MSLP was particularly low over 50–60°S, 30–80°E, with eight deep individual storms tracking eastward north of the sea ice zone in this sector. Nevertheless, the southerly component of the mean monthly wind field in this sector gave positive ice anomalies so that the overall contribution of this sector to the total ice loss was not exceptional.

Climatologically, Antarctic sea ice experiences its most rapid monthly retreat during December (Table 1); however, because of the very rapid retreat during spring, which left an SIE anomaly of -2.25×10^6 km^2 at the end of November and the lowest extent for that day in the satellite record, the overall December retreat was 0.63×10^6 km^2 less than usual. Nevertheless, during the early part of the month the absolute negative SIE anomaly became larger, attaining its greatest magnitude of -2.78×10^6 km^2 (3.36 SD below the mean) on 14 December, before decreasing to -1.68×10^6 km^2 (SD 2.19) by the end of the month. The December mean SAM index was -1.52, and there were further record negative MSLP anomalies off East Antarctica and over the northeast Weddell Sea. The anomalous northeasterly flow into the Weddell Sea resulted in further propagation of the polynya into the Weddell Sea, and this sector was responsible for 50% of the overall ice decrease for the month.

In 2017 the total SIE continued to have record low values for the day of the year until 9 April, although the rate of decrease varied considerably and the anomaly was very close to the values observed in previous years at some points. On average, the day of minimum SIE occurs on 20 February, but this can be up to 2 weeks earlier or later. In 2017 the minimum SIE of 2.07×10^6 km^2 occurred on 1 March, which was the lowest extent observed in the record, and the subsequent increase of SIE during March was slower than usual.

5. Discussion

The very rapid early melt season ice retreat that took place in the austral spring of 2016 coincided with a series of record atmospheric circulation anomalies over the 3 months. In September, a record deep ASL gave greater sea ice retreat than usual in the ABS and the Weddell Sea sectors, and since the maximum SIE for the year was in late August, this led to an overall September negative ice anomaly. In October amplified planetary waves and strong meridional flow led to strong poleward heat flux contributing to greater SIE retreat in the Ross Sea and Indian Ocean sectors. The most anomalous retreat took place in November, when ice loss in the Weddell Sea sector was double the climatological change, contributing an additional 0.76×10^6 km^2 to the retreat for the month. The springtime retreat was remarkable for the fact that the record sea ice diminishing atmospheric circulation anomalies occurred in different sectors of the Antarctic so that the overall anomaly built up throughout the spring months.

The atmospheric circulation at high southern latitudes was clearly anomalous in 2016, and there is a strong correlation between the marked periods of northerly atmospheric flow and ice retreat. However, the ocean will also have played a role in the loss of ice, although this is difficult to quantify. Sea surface temperatures over the Southern Ocean have increased by a few tenths of a degree since the late 1970s [*Liu and Curry*, 2010], and sea surface temperatures (SSTs) were particularly high close to the sea ice edge during late winter and spring 2016 (see https://data.giss.nasa.gov/gistemp/maps/). With the rapid retreat of sea ice in November a large area of open ocean was exposed at a time close to the maximum of incoming shortwave radiation. This will have increased the ocean temperature, inhibited the formation of new ice when air temperatures were below freezing and made the ice-albedo feedback particularly effective. High SSTs around the Antarctic persisted until the annual sea ice minimum in March and during the period of negative SIE anomalies immediately after the minimum.

While climate models project Antarctic SIE to decrease by around one third by the end of this century if greenhouse gas concentrations continue to increase [*Bracegirdle et al*., 2008], it is still too early to clearly identify the degree to which a longer-term background signal associated with increasing greenhouse gases is contributing to observed regional trends [e.g., *Hobbs et al*., 2015] and specific events such as the marked springtime SIE decrease in 2016. Our analysis has focused on shorter-term monthly variability and highlighted that this dominates over these timescales.

Acknowledgments
This work forms part of the Polar Science for Planet Earth program of the British Antarctic Survey and was supported financially by the UK Natural Environment Research Council under grant NE/K00445X/1. We are grateful to ECMWF for the provision of the ERA-Interim meteorological fields (available here: http://apps.ecmwf.int/datasets/data/interim-mdfa/) and to the U.S. National Snow and Ice Data Center for providing sea ice data (available here: http://nsidc.org/data/docs/daac/nsidc0079_bootstrap_seaice.gd.html). The usage of these data has been cited in the text and included within the reference list. We are grateful to Jeff Ridley of the UK Met Office for valuable comments on an early draft of this paper.

References

Bintanja, R., S. S. D. van Oldenborgh, B. Wouters, and C. A. Katsman (2013), Important role for ocean warming and increased ice-shelf melt in Antarctic sea-ice expansion, *Nat. Geosci.*, doi:10.1038/NGEO1767.

Bracegirdle, T. J., W. M. Connolley, and J. Turner (2008), Antarctic climate change over the twenty first century, *J. Geophys. Res.*, *113*, D03103, doi:10.1029/2007JD008933.

Bracegirdle, T. J., and G. J. Marshall (2012), The reliability of Antarctic tropospheric pressure and temperature in the latest global reanalyses, *J. Clim.*, *25*, 7138–7146.

Cavalieri, D. J., P. Gloersen, and W. J. Campbell (1984), Determination of sea ice parameters with the Nimbus-7 SMMR, *J. Geophys. Res.*, *89*, 5355–5369, doi:10.1029/JD089iD04p05355.

Dee, D. P., et al. (2011), The ERA-interim reanalysis: Configuration and performance of the data assimilation system, *Q. J. R. Meteorol. Soc.*, *137*, 553–597.

Ferreira, D., J. Marshall, C. M. Bitz, S. Solomon, and A. Plumb (2015), Antarctic ocean and sea ice response to ozone depletion: A two timescale problem, *J. Clim.*, *28*, 1206–1226.

Fetterer, F., K. Knowles, W. Meier, and M. Savoie (2002), *Sea Ice Index*, Natl. Snow and Ice Data Cent, Boulder, Colo., (Updated 2017). [Available at http://nsidc.org/data/g02135.html.]

Hall, A., and M. Visbeck (2002), Synchronous variability in the Southern Hemisphere atmosphere, sea ice, and ocean resulting from the annular mode, *J. Clim.*, *15*, 3043–3057.

Hawkins, E., and R. Sutton (2009), The potential to narrow uncertainty in regional climate predictions, *Bull. Am. Meteorol. Soc.*, *90*, 1095–1107.

Hobbs, W., N. L. Bindoff, and M. N. Raphael (2015), New perspectives on observed and simulated Antarctic sea ice extent trends using optimal fingerprinting techniques, *J. Clim.*, *28*, 1543–1560, doi:10.1175/JCLI-D-14-00367.1.

Holland, M., L. Landrum, Y. Kostov, and J. Marshall (2017), Sensitivity of Antarctic sea ice to the Southern Annular Mode in coupled climate models, *Clim. Dyn.*, doi:10.1007/s00382-016-3424-9.

Hosking, J. S., A. Orr, G. J. Marshall, J. Turner, and T. Phillips (2013), The influence of the Amundsen-Bellingshausen Seas low on the climate of West Antarctica and its representation in coupled climate model simulations, *J. Clim.*, *26*, 6633–6648.

Liu, J. P., and J. A. Curry (2010), Accelerated warming of the Southern Ocean and its impacts on the hydrological cycle and sea ice, *Proc. Natl. Acad. Sci. U.S.A.*, *107*, 14,987–14,992.

Marshall, G. J. (2003), Trends in the Southern Annular Mode from observations and reanalyses, *J. Clim.*, *16*, 4134–4143.

Marshall, G. J., and D. W. J. Thompson (2016), The signatures of large-scale patterns of atmospheric variability in Antarctic surface temperatures, *J. Geophys. Res. Atmos.*, *121*, 3276–3289, doi:10.1002/2015JD024665.

Parkinson, C. L., and J. C. Comiso (2013), On the 2012 record low Arctic sea ice cover: Combined impact of preconditioning and an August storm, *Geophys. Res. Lett.*, *40*, 1356–1361, doi:10.1002/grl.50349.

Parkinson, C. L., and N. E. DiGirolamo (2016), New visualizations highlight new information on the contrasting Arctic and Antarctic sea-ice trends since the late 1970s, *Remote Sens. Environ.*, *183*, 198–204.

Reid, P., S. Stammerjohn, R. Massom, T. Scambos, and J. Lieser (2015), The record 2013 Southern Hemisphere sea-ice extent maximum, *Ann. Glaciol.*, *56*, 99–106.

Serreze, M. C., and J. Stroeve (2015), Arctic sea ice trends, variability and implications for seasonal ice forecasting, *Phil. Trans. R. Soc. London Ser. A*, doi:10.1098/rsta.2014.0159.

Simmonds, I. (2015), Comparing and contrasting the behaviour of Arctic and Antarctic sea ice over the 35-year period 1979–2013, *Ann. Glaciol.*, *56*, 18–28.

Turner, J., T. J. Bracegirdle, T. Phillips, G. J. Marshall, and J. S. Hosking (2013a), An initial assessment of Antarctic sea ice extent in the CMIP5 models, *J. Clim.*, *26*, 1473–1484.

Turner, J., J. C. Comiso, G. J. Marshall, T. A. Lachlan-Cope, T. J. Bracegirdle, T. Maksym, M. P. Meredith, Z. Wang, and A. Orr (2009), Non-annular atmospheric circulation change induced by stratospheric ozone depletion and its role in the recent increase of Antarctic sea ice extent, *Geophys. Res. Lett.*, *36*, L08502, doi:10.1029/2009GL037524.

Turner, J., J. S. Hosking, T. Phillips, and G. J. Marshall (2013b), Temporal and spatial evolution of the Antarctic sea ice prior to the September 2012 record maximum extent, *Geophys. Res. Lett.*, *40*, 5894–5898, doi:10.1002/2013GL058371.

Turner, J., J. S. Hosking, T. J. Bracegirdle, G. J. Marshall, and T. Phillips (2015), Recent changes in Antarctic sea ice, *Phil. Trans. R. Soc. London Ser. A*, *373*, doi:10.1098/rsta.2014.0163.

Turner, J., J. S. Hosking, T. J. Bracegirdle, T. Phillips, and G. J. Marshall (2016), Variability and trends in the Southern Hemisphere high latitude, quasi-stationary planetary waves, *Int. J. Climatol.*, doi:10.1002/joc.4848.

Zachos, J. C., G. R. Dickens, and R. E. Zeebe (2008), An early Cenozoic perspective on greenhouse warming and carbon-cycle dynamics, *Nature*, *451*(7176), 279–283, doi:10.1038/nature06588.

Zhang, J. (2007), Increasing Antarctic sea ice under warming atmospheric and oceanic conditions, *J. Clim.*, *20*, 2515–2529.

Zhang, X., and J. E. Walsh (2006), Towards a seasonally ice-covered Arctic Ocean: Scenarios from the IPCC AR4 simulations, *J. Clim.*, *19*, 1730–1747.

Zwally, H. J., J. C. Comiso, C. L. Parkinson, D. J. Cavalieri, and P. Gloersen (2002), Variability of Antarctic sea ice 1979–1998, *J. Geophys. Res.*, *107*(C5), 3041, doi:10.1029/2000JC000733.